PHYSICAL REVIEW C VOLUME 15, NUMBER 1 JANUARY 1977

Common optical potential and peripheral processes between 1p-shell nuclei*

C. W. Towsley, P. K. Bindal, K.-I. Kubo,† K. G. Nair, and K. Nagatani
Cyclotron Institute, Texas A & M University, College Station, Texas 77843
(Received 20 September 1976)

Elastic and inelastic scattering were measured for beams of 100-MeV ^{10}B and 155-MeV ^{14}N on targets of ^{12}C and ^{16}O. These data and previously measured one-nucleon transfer data for the same four incident channels were analyzed simultaneously. A single set of optical potential parameters, fitting all the elastic scattering data, was obtained. Distorted-wave Born approximation analyses of the inelastic and transfer reactions were also done with this potential, resulting in good fits to the data. The common features in all of these peripheral collisions are emphasized.

[NUCLEAR REACTIONS NUCLEAR STRUCTURE ^{12}C(^{10}B, ^{10}B), ^{12}C(^{10}B, ^{10}B′), ^{16}O(^{10}B, ^{10}B), ^{16}O(^{10}B, ^{10}B′), E=100 MeV; ^{12}C(^{14}N, ^{14}N), ^{12}C(^{14}N, ^{14}N′), ^{16}O(^{14}N, ^{14}N), ^{16}O(^{14}N, ^{14}N′), E=155 MeV; measured $\sigma(\theta)$; optical potentials, EFR-DWBA analyses extracted β's.]

I. INTRODUCTION

Direct reactions produced in collisions between 1p-shell nuclei with incident energies around 10 MeV/nucleon have been studied in our laboratory. While much interesting information concerning reaction mechanisms and nuclear structure can be obtained from individual reactions,[1-3] it is also important to understand the systematics of these processes. For this purpose we consider the common features observed in various processes from four incident channels, namely 100-MeV ^{10}B and 155-MeV ^{14}N beams colliding with ^{12}C and ^{16}O targets.

It was noted that the elastic scattering angular distributions for these cases showed a typical diffraction pattern. This suggested that the gross features of such collisions can be understood in terms of simple wave optics without considering effects of detailed individual characteristics such as shell structure. Therefore an attempt was made to obtain a common optical potential that can fit all the cases.

The inelastic scattering data provide further evidence for the simple description where the individual structure does not have significant effects. In particular, the strong excitations of collective states (2^+ and 3^-) show similarities in these four different channels. Furthermore, the common potential is tested for one-nucleon transfer reactions in a reanalysis of data published previously[1] for these channels.

The single-nucleon transfer reactions induced by heavy ions occur predominantly in the nuclear periphery; hence they should be well explained by first-order distorted-wave Born approximation (DWBA). In fact, such analysis of more than 20 of the single-nucleon transfers seen in these experiments has already been performed, and excellent results were obtained.[1] In the present work, only a few examples of single-nucleon transfers will be discussed in the context of the common optical potential.

II. EXPERIMENTAL PROCEDURE

The details of the experimental procedures are not presented here as they are described elsewhere.[1] The incident $^{10}B^{3+}$ and $^{14}N^{4+}$ beams were obtained from the Texas A&M University cyclotron. Natural ^{12}C foil targets of 200–400 μg/cm^2 and a gas target with enriched ^{16}O operating at a pressure of 100–200 Torr were used. The counter telescopes typically consisted of about 50, 50, and 2000 μm for ΔE_1, ΔE_2, and E, respectively. Typical energy resolution was 400–500 keV, mainly due to kinematic broadening. A multiple Gaussian peak fitting program was utilized to extract peak areas even though the energy resolution was good enough to separate the peaks adequately. The estimated errors in absolute cross sections are ~20%, while statistical errors are quite small as indicated in the individual results below. Uncertainties in the absolute angle reading were estimated to be less than $\pm 0.2^\circ$ in the laboratory, while errors in the relative angles in a given angular distribution are believed to be much smaller than that.

III. ELASTIC SCATTERING

The experimental elastic scattering angular distributions are shown in Fig. 1(a). In these cases, the Fraunhofer approximation should be applicable as in these scattering processes the Sommerfeld constant $\eta \sim 2$ and $kR \sim 30$ ($\eta \ll kR$). Thus these diffraction patterns are quite understandable. Under

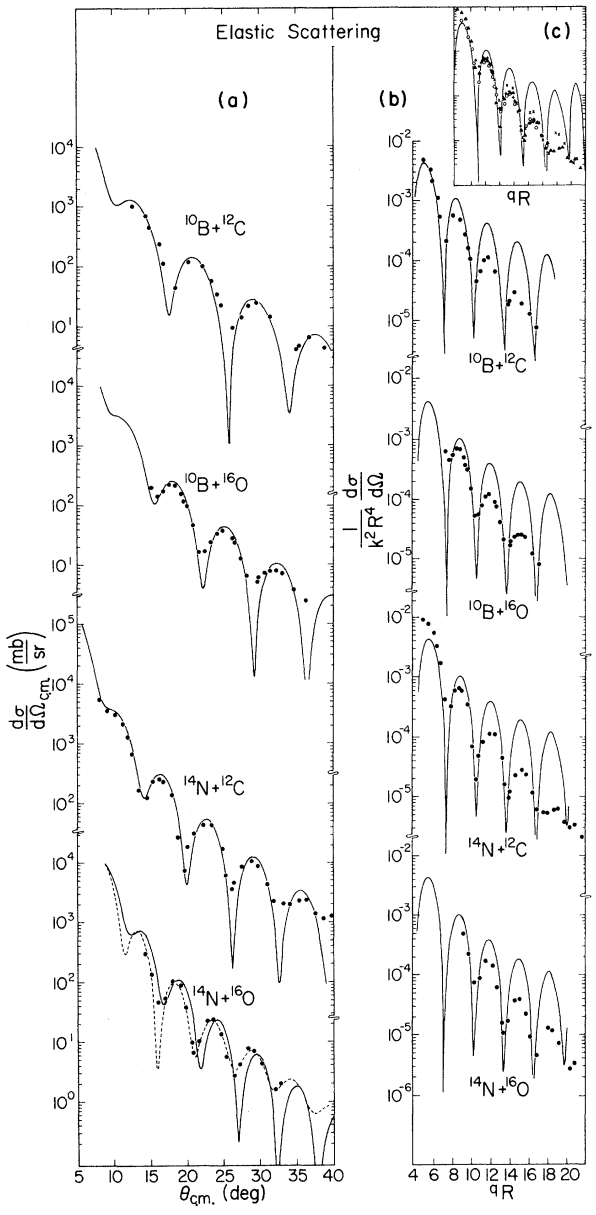

FIG. 1. Angular distributions of elastic scattering: (a) the experimental points are compared to the optical potential model fits, i.e., the solid curves show the results of the common potential (Set A in Table I), while the dashed curve in the $^{14}N+^{16}O$ channel shows the fits using the different diffusenesses ($a_r = 0.80$ fm and $a_i = 0.47$ fm). (b) The experimental points are compared to the Blair model fits shown by the solid curves. (c) All results in (b) are displayed together with the universal curve to show their similarity.

such conditions, it is also expected that the processes involved are insensitive to the details of nuclear structure. This in turn suggests that all these four cases should follow a similar scattering mechanism, and that the apparent differences in the experimental angular distributions are only due to kinematical differences of masses and energies and geometrical difference of nuclear sizes. The angular distributions are thus replotted using momentum transfer q, so that these dependences are minimized. The results, shown in Fig. 1(b), explicitly show their similarities not only in phases of oscillations but also in magnitudes [see also Fig. 1(c)]. In fact, such diffraction features should be well explained by the Blair model,[4] where the differential cross section is related to the simple analytical form (the so-called "universal" curve[4])

$$\frac{1}{k^2R^4}\frac{d\sigma}{d\Omega}=\frac{J_1^2(qR)}{(qR)^2}, \tag{1}$$

where the notations are standard. The comparisons to the experimental data are displayed in Fig. 1(b) with the curves. The locations of maxima and minima as well as the magnitude at forward angles are reproduced quite accurately as expected. The slower decrease of the theory with angle is due to the sharp-edge assumption of the model. Such general agreement obtained indicates that this type of nucleus-nucleus collision is indeed insensitive in its gross features to the microscopic details of the nuclear structure.

This similarity in turn suggests the existence of a common optical potential that could explain all these four cases. Furthermore, if it is found, such a potential should be applicable to other systems under similar conditions due to this insensitivity to the individual structure. It should also be pointed out that finding of such a common potential is quite useful in practice since optical potentials are always needed in various reaction calculations, e.g., the DWBA calculation and the compound nuclear Hauser-Feshbach calculation. It is especially useful in systems where unstable nuclei are involved for which experimental data on elastic scattering cannot be obtained. Therefore a search was carried out to find such a set of parameters. A Woods-Saxon potential with volume absorption and with the Coulomb part corresponding to that of a uniformly charged sphere was used. A modified version of the computer code JIB6[5] was utilized with the usual minimization of χ^2. In the actual search, the Coulomb radius parameter r_c was kept a constant 1.20 fm for simplicity, resulting in a six-parameter search.

Different sets of potentials differing widely in depths and other parameters have been found to fit the elastic scattering data of several similar heavy-ion systems.[1,6,7] It has been found often that the real depth of 100 MeV provides good fits. Therefore, fixing $V_0 = 100$ MeV, we obtained a set of parameters given in Table I (Set A), which fits all four channels. The fits to the individual cases

TABLE I. Optical potential parameters. The potential is given as

$$U(r) = -V\frac{1}{1+\exp[(r-R_r)/a_r]} - iW\frac{1}{1+\exp[(r-R_i)/a_i]} + V_c\,,$$

where $R = r(A_1^{1/3}+A_2^{1/3})$ and V_c is the Coulomb potential for a uniformly charged sphere with $r_c = 1.20$ fm. In the Set A, a better fit for the (^{14}N+^{16}O) channel was obtained by changing $a_r = 0.80$ fm and $a_i = 0.47$ fm (see text). The χ^2 for all these fits were less than 10, typically ~2.

Set	Channel	V (MeV)	r_r (fm)	a_r (fm)	W (MeV)	r_i (fm)	a_i (fm)
A	Common (all 4)	100.0	0.97	0.65	40.0	1.18	0.45
B	^{10}B+^{12}C	44.7	1.04	0.72	15.0	1.33	0.37
	^{10}B+^{16}O	54.5	1.09	0.72	15.0	1.31	0.37
	^{14}N+^{12}C	59.1	1.02	0.80	15.0	1.23	0.70
	^{14}N+^{16}O	54.9	1.06	0.84	18.6	1.28	0.60

are shown in Fig. 1(a) as solid lines. As seen, all these data were fitted quite well except possibly for the ^{14}N on ^{16}O case. It should be pointed out that the experimental cross section was measured with a finite angular acceptance (typically $\Delta\theta_{\text{c.m.}} \simeq 0.6°$), while the theoretical curves were not corrected for this effect. Thus the discrepancies seen at the sharp minima should not be taken seriously. These successful fits ensure that the gross features are governed by the scattering dynamics. Because of the insensitivity on the microscopic structure of the nuclei involved, the potential should be applicable to systems of similar masses and energies. In fact such tests were made, and two examples are presented here. The angular distributions[8] of 59-MeV ^{6}Li on ^{12}C and 100-MeV ^{10}B on ^{14}N elastic scattering[9] were analyzed by the

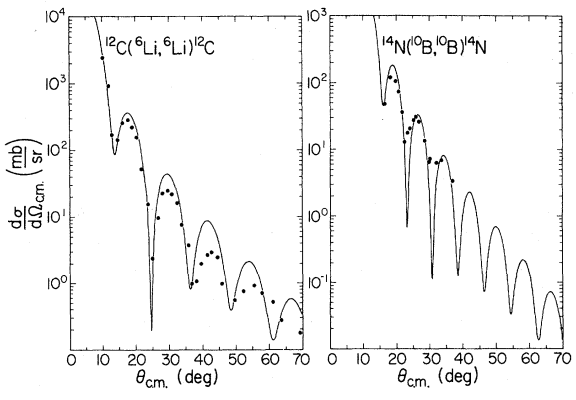

FIG. 2. Optical model fits using the common potential (Set A in Table I) to two additional systems. The data points are from Refs. 8 and 9 and the calculated results are shown by the solid curves.

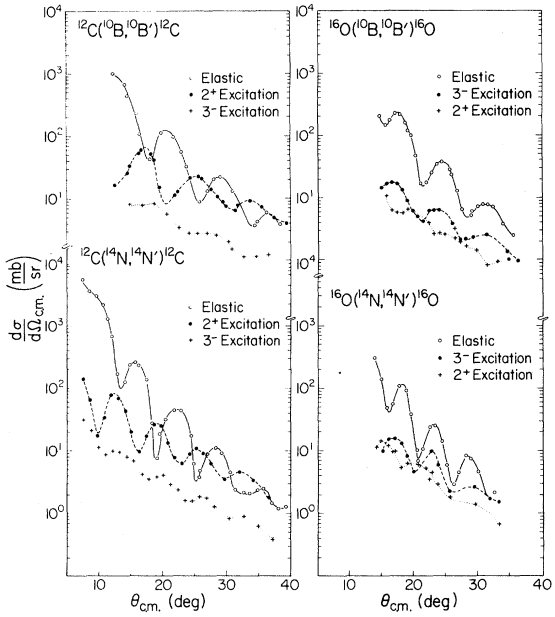

FIG. 3. Angular distributions of inelastic scattering. The data are shown together with the elastic scattering for comparisons. The lines are drawn through the points to guide the eye.

present common potential and comparisons to the data are displayed in Fig. 2. The calculated results agree well with the data, except for the backward angles in ^{6}Li scattering where even a more careful study[8] encountered a similar problem. In the case of ^{14}N on ^{16}O, where the fit to the data was not good, a further search was made to improve it. It was found that changes in the diffuseness parameters to $a_r = 0.80$ fm and $a_i = 0.47$ fm improved the fits, seen in Fig. 1(a) as dashed lines.

As usual, it is not claimed here that these potentials are unique solutions; therefore additional attempts were made to search for a completely different family of potentials. Another family of potentials was adopted with the real depth of ~50 MeV and the imaginary depth of ~15 MeV. The six-parameter search was conducted first to find a common potential as in the case of the deeper potential above. The search, however, never converged to one set of parameters. It provided instead individual fits with slightly different sets of parameters listed as Set B in Table I. The fits to the data are as good as those obtained with the potentials A.

IV. INELASTIC SCATTERING

We expect that the inelastic transitions to collective states also should show strong diffractive features as in the elastic scattering discussed. It

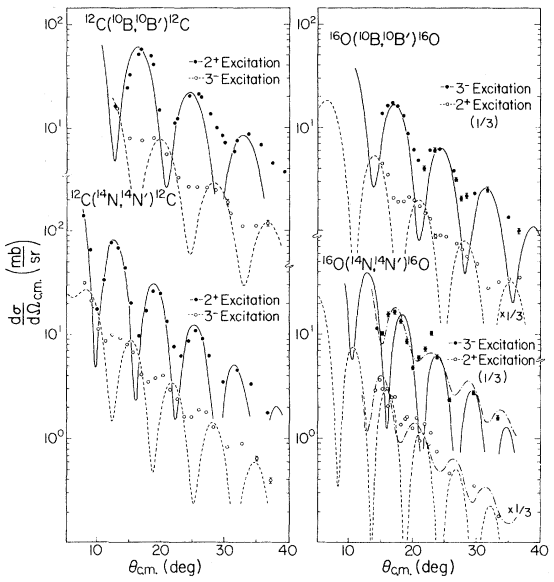

FIG. 4. Angular distributions of inelastic scattering and Austern-Blair fits: The Austern-Blair calculations are compared to the data. The strengths extracted from these comparisons are listed in Table II.

can be assumed again that the process is quite insensitive to the choice of projectile nucleus. Thus we consider the inelastic excitations of ^{12}C to the 2^+ state at 4.44 MeV and the 3^- state at 9.63 MeV, and those of ^{16}O to the 3^- state at 6.13 MeV and 2^+ state at 6.92 MeV with the ^{10}B and ^{14}N projectiles. The angular distributions are shown in Fig. 3, together with elastic scattering for comparisons. They indeed show strong oscillations, and in particular the transitions to the 2^+ state in ^{12}C and the 3^- state in ^{16}O demonstrate the well-known Blair phase rules[4] in their angular distributions compared to those of the elastic scattering. The patterns are not quite so demonstrative in the transition to the 3^- state in ^{12}C and the 2^+ state in ^{16}O, where the oscillations are also damped. In fact, the 3^- excitation in ^{12}C by ^{14}N is almost out of phase with the elastic angular distribution. In these latter two transitions, however, it is expected that the processes are not so simple as in the former two cases, since the residual states are considered less collective and a simple macroscopic description for these states may not be adequate. Nevertheless, we carry out the analyses for these transitions also.

Before the analyses of the DWBA are discussed, the application of a simpler model is considered. Austern and Blair[4,10] derived a simplified treatment of the DWBA calculation. The radial overlap integral in the DWBA is replaced by the derivative of the amplitude of the scattering waves η_l, i.e.,

$$\int_0^\infty dr f_l(k,r)\frac{\partial V}{\partial r} f_l(k,r) = \frac{iE}{2k}\frac{\partial \eta_l}{\partial R},$$

where, in the overlap integral of the left side, f_l is the radial part of the partial scattering wave and $\partial V/\partial r$ is the usual form factor. For the purpose of the analyses here, it is not necessary to adopt this simplified treatment, since the full calculation of the DWBA is carried out. However, it was considered worthwhile to examine the model for the present cases, because there have been very few attempts of application of the model to heavy-ion-induced processes. And the validity of such a model together with the common potential will ensure easy access to analyses and predictions of heavy-ion inelastic scattering in general.

The real advantage of the model lies in the fact that the calculation can be made using very simple forms for η_l such as the parametrization of the reflection coefficients. We used, however, the numerical amplitudes calculated from the optical potential described in the elastic scattering cross section. Some of the results are shown in Fig. 4. The theoretical calculations are seen to reproduce the experimental results for the more collective states reasonably well. The success of these fits again confirms the argument that the general features of these collisions can be treated in a quite simple manner. Attempts were also made for ex-

TABLE II. Extracted deformation lengths (βR values).

		Residual states			
		^{12}C		^{16}O	
Analysis	Projectile	2^+	3^-	3^-	2^+
Austern-Blair	^{10}B	1.4	0.8	0.7	0.8
	^{14}N	1.2	0.5	0.5	0.7
DWBA[a]	^{10}B	1.5, 1.8	0.8, 1.0	0.9, 1.1	0.7, 0.8
	^{14}N	1.2, 1.5	0.6, 0.7	0.9, 1.1	0.6, 0.8
Previous values[b]		1.1–1.8	0.7–1.1	0.9–2.4	0.6–0.8

[a] Two values quoted are the results using the real and imaginary radii, respectively.
[b] References 11, 12, 13, and 14.

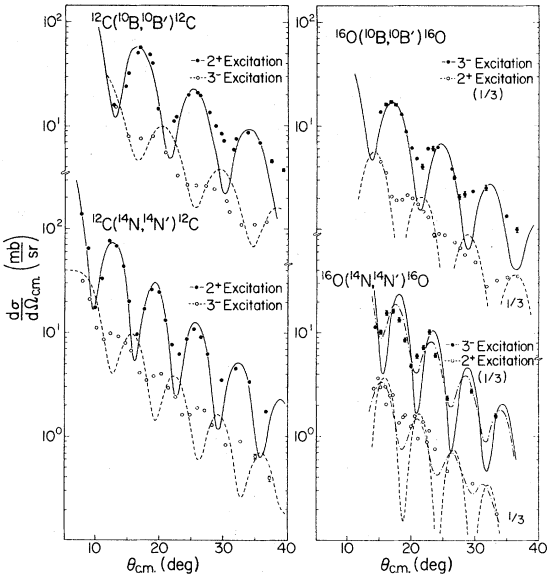

FIG. 5. Angular distributions of inelastic scattering and DWBA fits: The DWBA results using the common potential (Set *A* in Table I) are compared to the data. The strengths extracted from these comparisons are listed in Table II. The dash-dot line in the $^{16}O(^{14}N, ^{14}N')$ ^{16}O case is the result using the different diffusenesses ($a_r = 0.80$ fm and $a_i = 0.47$ fm).

tracting the absolute strengths. The comparisons to the experimental results yield the deformation lengths βR and the results are summarized in Table II. As seen, the present results are in good agreement with earlier results in the literature.[11-14]

The DWBA analyses with macroscopic complex form factors were carried out using the common potential derived in the previous section. Since the procedure is very straightforward and well known, no description is given here. The fits to the data are displayed in Fig. 5. It can be seen that the 2^+ state in ^{12}C and the 3^- state in ^{16}O are fitted quite well, while the 3^- state in ^{12}C and the 2^+ state in ^{16}O are almost out of phase with the calculated angular distributions. As mentioned above, the complexities in the excitation of the latter two cases remain for further study. In fact, such difficulties were noted in similar DWBA analyses of ^6Li scattering[12] and in the more sophisticated analyses of ^{14}N scattering using the double-folding method.[14] With these fits, we obtained the deformation lengths βR which are listed in Table II. Two values are quoted, depending on the choice of the real or imaginary radius. It is seen that the present results are in good agreement with the previously known values. This successful result shows that the common potential is good for the analysis of these inelastic scatterings. It should be emphasized that the inelastic scattering is sensitive to the potential in a different manner from the elastic scattering. Therefore, a successful fit is not automatically obtained by using the potential which fits the elastic scattering. This different response from the potential used is much more amplified[1] in the analysis of transfer reactions, since the process takes place in a very localized region near the surface and the detailed behavior of the distorted waves generated from the common potential becomes even more critical.

V. ONE-NUCLEON TRANSFER REACTIONS

Systematic studies of proton and neutron transfer reactions from these incident channels were made for more than twenty transitions.[1] The exact finite range (EFR) DWBA analyses yielded in general very successful results. Here we intend only to test the present optical potentials for these transfer channels. Examples of such calculations using the common potential *A* are shown in Fig. 6. One transition from each incident channel is presented as an example. As seen in the figure, good fits to the experimental results are obtained in their shapes; all spectroscopic factors calculated showed satisfactory agreement (within a factor of 2) to various known values just as described in detail in Ref. 1. It is thus concluded that the present common potential provides satisfactory descriptions for various one-nucleon transfer channels also. Considering the stringent criteria for the fits for transfer reactions this can be taken as additional evidence for the goodness of the common

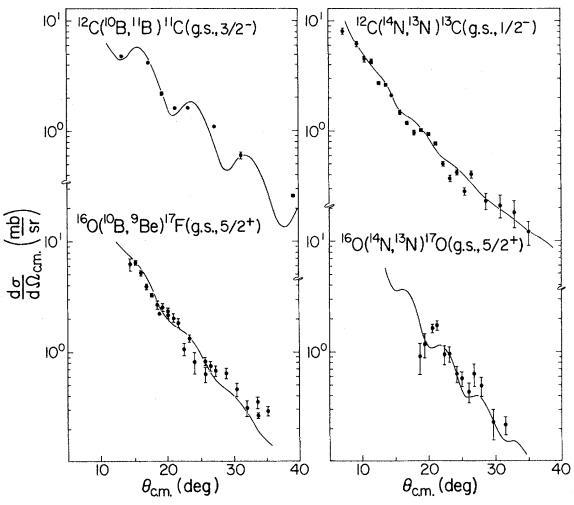

FIG. 6. Angular distributions of one-nucleon transfer reactions and EFR-DWRA fits: The transitions are to the ground states as indicated. The EFR-DWBA results using the common potential (Set *A* in Table I) are shown by the solid curves.

potential.

The potential sets B were also tested for these transfer reactions. The calculated results are quite similar to those using the potential set A in the angular regions studied here. However, it was found that in the backward angles there were differences. The potential B produces a secondary maximum in the angular distribution at certain backward angles which yields a somewhat plateau-like pattern. Such behavior can be understood theoretically when a potential has a weak absorption and a shallow real depth.[15] Unfortunately, differences in the calculated results using these two types of potentials A and B appear beyond the angle ranges of the present measurements. Although experimental measurements become difficult due to the drastic reductions of reaction yields in backward angles, studies of the backward angles are certainly desired.

VI. SUMMARY

Experimental results of the elastic scattering of four heavy-ion systems were collectively analyzed. In the present dynamical situation of about 10 MeV/nucleon incident energies between light nuclei, the Fraunhofer-type diffraction pattern dominates the elastic scattering and details of the microscopic structure of the colliding nuclei are not noticeable. A common optical potential was thus found to reproduce these data quite well. Moreover, two additional elastic scattering data were also fitted. The macroscopic DWBA analyses using the common potential seem to give a fair description of the inelastic excitations of the 2^+ and 3^- states in ^{12}C and ^{16}O. In detail, however, the present DWBA calculations could not reproduce the transitions to the second-excited states as previously noted. The common potential also produced good results when it was applied to one-nucleon transfer channels in the EFR-DWBA calculations.

It will be interesting and useful to extend the present analysis to a greater variety of incident systems. It is also desirable to extend this systematic analysis to more exit channels such as multinucleon transfer reactions and compound processes. Possible deviations from such common features stressed here, if observed, will certainly extend the understanding of nucleus-nucleus collisions.

We wish to thank our colleagues M. Hamm and R. Hanus for their help in various phases of the work.

[1]K. G. Nair, H. Voit, C. W. Towsley, M. Hamm, J. D. Bronson, and K. Nagatani, Phys. Rev. C 12, 1575 (1975).

[2]K. Nagatani, D. H. Youngblood, R. Kenefick, and J. Bronson, Phys. Rev. Lett. 31, 250 (1973); M. Hamm, C. W. Towsley, R. Hanus, K. G. Nair and K. Nagatani, *ibid.* 36, 846 (1976).

[3]N. Anyas-Weiss, J. C. Cornell, P. S. Fisher, P. N. Hudson, A. Menchaca-Rocha, D. J. Millener, A. D. Panagiotou, D. K. Scott, D. Strottman, D. M. Brink, B. Buck, P. J. Ellis, and T. Engeland, Phys. Rep. 12C, 201 (1974).

[4]J. S. Blair, Lectures in Theoretical Physics, University of Colorado, Boulder, VIII C, 1965 (unpublished), p. 343; J. S. Blair, G. W. Farwell, and D. K. McDaniels, Nucl. Phys. 17, 641 (1960).

[5]G. M. Lerner (unpublished).

[6]W. von Oertzen, M. Liu, C. Caverzasio, J. C. Jacmart, F. Pougheon, M. Riou, J. C. Roynette, and C. Stephen, Nucl. Phys. A143, 34 (1970).

[7]R. M. DeVries, M. S. Zisman, J. G. Cramer, K. L. Liu, F. D. Becchetti, B. G. Harvey, H. Homeyer, D. G. Kovar, J. Mahoney, and W. von Oertzen, Phys. Rev. Lett. 32, 680 (1974).

[8]H. G. Bingham, M. L. Halbert, D. C. Hensley, and E. Newman, Phys. Rev. C 11, 1913 (1975).

[9]Data measured at this laboratory.

[10]N. Austern and J. S. Blair, Ann. Phys. 33, 15 (1965).

[11]G. R. Satchler, Nucl. Phys. A100, 497 (1967); F. Hinterberger, G. Mairle, U. Schmidt-Rohr, G. J. Wagner, and P. Turek, *ibid.* A115, 570 (1968).

[12]P. K. Bindal, K. Nagatani, M. J. Schneider, and P. D. Bond, Phys. Rev. C 9, 2154 (1974).

[13]B. G. Harvey, J. R. Meriweather, J. Mahoney, A. Bussiere de Nercy, and D. J. Horen, Phys. Rev. 146, 712 (1966); G. M. Crawley, and G. T. Garvey, *ibid.* 160, 981 (1967); G. G. Duhamel, H. Langevin-Joliot, J. P. Didelez, E. Gerlic, and J. Van de Wiele, Nucl. Phys. A231, 349 (1974).

[14]P. J. Moffa, J. P. Vary, C. B. Dover, C. W. Towsley, R. G. Hanus, and K. Nagatani, Phys. Rev. Lett. 35, 992 (1975).

[15]K. W. Ford and J. A. Wheeler, Ann. Phys. 7, 259 (1959); N. K. Glendenning, Rev. Mod. Phys. 47, 659 (1975).